

CFD-MODELLING OF SELECTIVE NON-CATALYTIC REDUCTION OF NO_x IN GRATE-KILN PLANTS

Per E. C. BURSTRÖM[†], T. Staffan LUNDSTRÖM[†], B. Daniel MARJAVAARA^{††} and Simon TÖYRÄ^{††}

[†]Division of Fluid Mechanics, Luleå University of Technology, SE-971 87 Luleå, SWEDEN

^{††}LKAB, SE-981 86 Kiruna, SWEDEN

*Corresponding author, E-mail address: per.burstrom@ltu.se

ABSTRACT

The overall goal of this project is to find out if selective non-catalytic reduction (SNCR) technologies can be used in grate-kiln plants for NO_x reduction. The technique has, to the best knowledge of the authors, never been used in this context before despite that it is commonly used in cement and waste incineration plants.

A Computational Fluid Dynamic model of parts of a real grate was created and numerical simulations with a commercial code was carried out solving the flow field. A model for spray injection into the grate was then included in the model enabling a study of the overall mixing between the injected reagent droplets and the NO_x polluted air. The simulations show promising results for SNCR with urea but not with ammonia.

NOMENCLATURE

| | |
|-----------|-----------------------|
| λ | thermal conductivity |
| μ | dynamic viscosity |
| ρ | density |
| c_p | specific heat |
| p | pressure |
| Q | heat transfer rate |
| u | velocity |
| V | heat of vapourisation |

INTRODUCTION

In this paper the flow in a part of a grate in an iron ore pelletizing plant is modeled with Computational Fluid Dynamics (CFD) with the aim to investigate methods to reduce emissions of NO_x. Of particular interest is injection of Ammonia or Urea with a technique called selective non-catalytic reduction (SNCR).

LKABs main business is iron-ore mining. The first stage in making iron ore pellets is the mining of the ore, where the ore has been processed in the sorting plant through primary crushing to separate the waste rock from the ore. In a second stage the ore is ground down in several stages in a concentration plant to a slurry and separated with the use of magnetic separators to filter out unwanted components. Then the ore slurry is pumped to the pelletizing plant, where it is drained with help of filters and mixed with different binders and additives. The mixture is then feed into balling drums where the ore is rolled into balls. The balls are recycled through the drums until they have the right size, which is about 0.01 m in diameter, thereafter the green pellets are loaded into the grate-kiln.

The four steps in the grate-kiln process are: drying, heating, firing, and cooling, see Figure 1. In the first step the green pellets are dried by forcing air through the pellet bed first upwards, Up Draught Drying (UDD) then downwards, Down Draught Drying (DDD). In the second step the green pellets are heated in the Tempered Preheat (TPH) from about 400°C to about 1000°C. After this the temperature is increased to about 1100°C in the Preheat (PH), which is the last zone in the grate and it is where the green pellets oxidize from magnetite to hematite. In a third step the green pellets are fed into a rotating kiln in which the temperature is about 1250°C in order to sinter the green pellets and give them their hard surface needed for production and transportation. In the last step the pellets are cooled down in an annular circular cooler which consists of four zones each supplying the rest of the system with heated air.

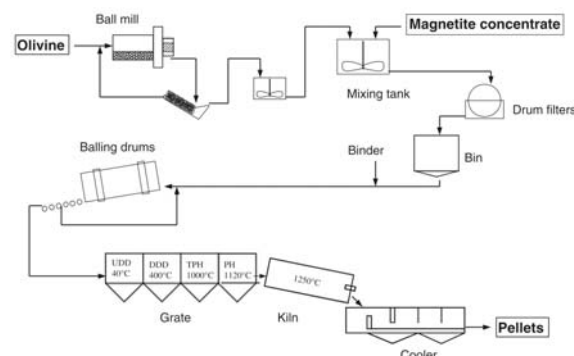


Figure 1: Flow scheme for a typical pelletizing plant.

The energy to the process is partly generated by oxidation of the pellets but also partly supplied by a coal burner in the rotating kiln. From this burner several emissions are released including nitrogen oxides. The regulations of such emissions are becoming tougher at the same time as the production rate is anticipated to increase. Hence there is a need to reduce the fraction of emissions per tons of pellets produced. One way of doing this is to use reagents to reduce the emission of NO_x by the SNCR-technique. Obviously this must be done without reducing the production and affecting the quality of the pellets. The principle of the SNCR process is rather simple. A fluid reagent of a nitrogenous compound is injected into, and mixed with, the hot gas. The reagent then, reacts with the NO_x converting it to nitrogen gas and water vapor. SNCR is selective since the reagent reacts mainly with NO_x, and not with other major components of the gas.

Nothing has to the authors knowledge been published on NO_x reduction by the usage of SNCR in grate-kiln plants, but the technique is commonly applied in cement and waste incineration plants. The cement process is characterized by higher temperatures in the kiln with resulting NO_x emissions, but often with a more optimal temperature, oxygen level and residence time in the volume of interest for the SNCR than in the grate-kiln process. It has been found that the temperature, the NO_x profile and the extent of mixing between the reagent and the flue gases are important variables for a successful installation of the SNCR technique (Javed et al., 2007). Also the resident time within a predefined temperature window is essential. All of this must be full-filled in order to get a good reduction.

In what follows the theoretical setup of the reagents and the reactions are presented. Then the geometry, mesh and the settings used for the simulations of the flow are outlined. Thereafter follows the result, which are finally discussed and concluded.

THEORY

Urea Evaporation

Urea evaporation/decomposition is not fully understood and several assumptions need to be done. Following Birkhold et al. (2007) the first is that the aqueous urea is assumed to heat up to the boiling point at which the water evaporates. When all the water is gone the thermal breakdown of the urea is initiated according to:

- 1) (NH₂)₂CO(aq) → (NH₂)₂CO(l) + H₂O(g)
- 2) (NH₂)₂CO(l) → (NH₂)₂CO(g)
- 3) (NH₂)₂CO(g) → NH₃(g) + HNCO(g).

The liquid evaporation model used handles the evaporation of the water in the first step. In the second step the rate is assumed to follow the subsequent relationship:

$$1 \cdot 10^{12} \cdot e^{-V/RT_d} \text{ 1/s} \quad (1)$$

where the heat of vaporisation V is set to, 87.4 kJ/mol (Birkhold et al., 2007).

For aqueous ammonia the evaporation of the water is derived by the liquid evaporation model and the ammonia mass transfer by the Ranz-Marshall correlation.

Water Evaporation

The temperature of the injected droplets is controlled by both the convective heat transfer with the flue gases from the rotating kiln and the transfer coupled with the latent heat of vaporization. The convective heat transfer is modelled with the following expression:

$$Q_c = \pi d \lambda_g Nu (T_g - T_d) \quad (2)$$

where d is the droplet diameter, λ the thermal conductivity and T the temperature. The subscripts g and d refer to the continuum gas phase and the droplet, respectively. The Nusselt number, Nu , is calculated by the empirical formula correlated by Ranz and Marshall:

$$Nu = 2 + 0.6 Re^{1/2} Pr^{1/3}, \quad (3)$$

where the Prandtl number is defined as:

$$Pr = \frac{\mu_g c_{p,g}}{\lambda_g} \quad (4)$$

where μ_g is the dynamic viscosity and $c_{p,g}$ is the specific heat capacity. The Reynolds number is calculated from the slip velocity in the following way:

$$Re = \frac{\rho_g (|u| - |u_d|) d}{\mu_g} \quad (5)$$

where $|u|$ is the gas velocity and $|u_d|$ is the droplet velocity.

The evaporation of the water in the urea-water droplet is estimated with a liquid evaporation model. The model chooses one of two mass transfer correlations depending on if the droplet has reached the boiling point or not. The boiling point is determined by the Antoine equation:

$$p_{sat} = p_{ref} \exp \left(A - \frac{B}{T+C} \right) \quad (6)$$

where A , B and C are empirical coefficients. If the vapour pressure is higher than the gaseous pressure the droplet is assumed to boil and the mass transfer is determined by the latent heat of vaporization:

$$\frac{dm}{dt} = \dot{m} = -\frac{Q_c}{V} \quad (7)$$

where V is the latent heat of evaporation and Q_c is the convective heat transfer. If the droplet is below the boiling point the mass transfer is given by:

$$\frac{dm}{dt} = \dot{m} = \pi d D_g Sh \frac{W_c}{W_g} \log \left(\frac{1-X}{1-X_g} \right) \quad (8)$$

where the subscript g refers to the gas continuum mixture surrounding the droplet and the subscript c denote the gas-phase properties of the evaporating component. The variable W is the molecular weight, d is the droplet diameter, D is the dynamic diffusivity and X is the molar fraction.

The Sherwood number is calculated as:

$$Sh = 2 + 0.6 Re^{1/2} Sc^{1/3} \quad (9)$$

where the Schmidt number is calculated from:

$$Sc = \frac{\mu_g}{\rho_c D_c} \quad (10)$$

The model does not account for condensation hence the mass transfer rate in Equation (8) can only be negative and the current version of the model is only suitable for one component of mass transfer.

For the simulation with urea a modified version of the liquid evaporation model is used which is considered to be used when evaporating oil droplets, see (Ansys CFX-Solver Theory Guide, 2006). This is done since the multiphase reaction mechanism for urea and the modified version of the liquid evaporation model uses similar approaches to calculate averaged properties.

SNCR Chemistry

Ammonia and Urea are commonly used as reagents in the SNCR process to reduce NO emissions with a rather narrow temperature window for a high efficiency, 870-1150°C. The advantage of urea as compared to ammonia is easier handling and storage of the reagent. Experimental observations (Rota et al., 2002; Alzueta et al., 1998) have furthermore shown that the temperature window for efficient use of urea is, as compared to ammonia, shifted towards higher temperatures with the same ratio between the nitrogen in the reagent used and the NO in the emission gases.

The reaction rate, regardless of reagent, is modeled by the Arrhenius equation:

$$k = AT^b \exp(-E/RT) \quad (11)$$

where A is the pre-exponent, b the temperature exponent, E the activation energy and R the universal gas constant. The model used for the SNCR chemistry is developed by Brouwer et al. (1996) and is a seven-step reduced kinetic mechanism that is outlined in Table 1, where the ammonia pathway is described by the first two reactions. An often used assumption is that the decomposition of urea in a SNCR process is instantaneous (Brouwer et al., 1996; Nguyen et al., 2008). In this work, however, the proposed two-step model from Rota et al. (2002) is applied. In this model urea is decomposed into ammonia and HNCO as shown in Table 2.

Table 1: Seven step reduced kinetic SNCR mechanism^a.

| | Reaction | A | b | E |
|--------------------|--|----------|------|------------|
| Brouwer reaction 1 | $\text{NH}_3 + \text{NO} \rightarrow \text{N}_2 + \text{H}_2\text{O} + \text{H}$ | 4.24E+02 | 5.30 | 349937.06 |
| Brouwer reaction 2 | $\text{NH}_3 + \text{O}_2 \rightarrow \text{NO} + \text{H}_2\text{O} + \text{H}$ | 3.50E-01 | 7.65 | 524487.005 |
| Brouwer reaction 3 | $\text{HNCO} + \text{M} \rightarrow \text{H} + \text{NCO} + \text{M}$ | 2.40E+08 | 0.85 | 284637.8 |
| Brouwer reaction 4 | $\text{NCO} + \text{NO} \rightarrow \text{N}_2\text{O} + \text{CO}$ | 1.00E+07 | 0 | -1632.4815 |
| Brouwer reaction 5 | $\text{NCO} + \text{OH} \rightarrow \text{NO} + \text{CO} + \text{H}$ | 1.00E+07 | 0 | 0 |
| Brouwer reaction 6 | $\text{N}_2\text{O} + \text{OH} \rightarrow \text{N}_2 + \text{O}_2 + \text{H}$ | 2.00E+06 | 0.0 | 41858.5 |
| Brouwer reaction 7 | $\text{N}_2\text{O} + \text{M} \rightarrow \text{N}_2 + \text{O} + \text{M}$ | 6.90E+17 | -2.5 | 271075.646 |

Table 2: Two-step urea decomposition model^a.

| Reaction | A | b | E |
|--|----------|---|-----------|
| $\text{CO}(\text{NH}_2)_2 \rightarrow \text{NH}_3 + \text{HNCO}$ | 1.27E+04 | 0 | 65048.109 |
| $\text{CO}(\text{NH}_2)_2 + \text{H}_2\text{O} \rightarrow 2\text{NH}_3 + \text{CO}_2$ | 6.13E+04 | 0 | 87819.133 |

To deal with the radicals in the reactions a couple of assumptions of equilibrium are introduced (Westbrook et al., 1984; Baulch et al., 1992; Löffler et al., 2005):

$$2\text{OH} + \text{M} \leftrightarrow \text{O} + \text{H}_2\text{O} + \text{M}, \text{ which gives}$$

$$[\text{OH}] = 212.9 \text{ T}^{-0.57} \text{ e}^{-4595/\text{T}} [\text{O}]^{1/2} [\text{H}_2\text{O}]^{1/2} \text{ mol/m}^3$$

^a Units of A are m-mol-s-K for E units are J/mol.

and the O approach is according to (Warnatz, 1990; Löffler et al., 2005):

$$\text{O}_2 + \text{M} \leftrightarrow \text{O} + \text{O} + \text{M}, \text{ resulting in}$$

$$[\text{O}] = 36.64 \text{ T}^{1/2} \text{ e}^{-27123/\text{T}} [\text{O}_2]^{1/2} \text{ mol/m}^3$$

where [] denote molar concentration.

CFD MODELLING

Now that the details about the reagents and the reactions are sorted out the CFD model will be described. ANSYS CFX11 was used for the numerical simulations. In this study a virtual model of the PH/TPH-zone in the grate is built since the reagents will be injected in this section of the process. To reduce the usage of CPUs only a part of the kiln and the air channel into the TPH-zone are modeled, see Figure 2. The heated polluted flue gases from the burner enter into the PH-zone from the kiln.

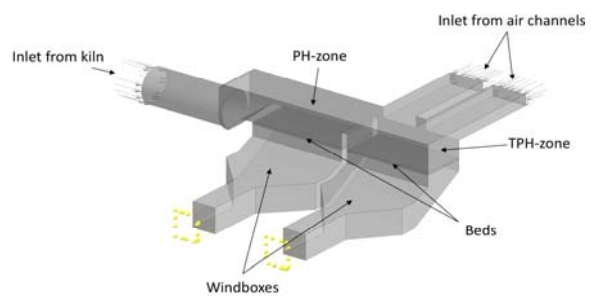


Figure 2: Model of PH- and TPH-zone including the pellet bed.

Mesh

The mesh used consists of 943k nodes, see Figure 3. The mesh is designed to be coarser after the bed in the windboxes and is refined in the bed and close to the injection points. In the mesh used, the boundary layer is not resolved again with the aim to keep the usage of CPUs on a relevant level. This is a crude assumption but it is believed that it will not influence the bulk flow to any large extent.

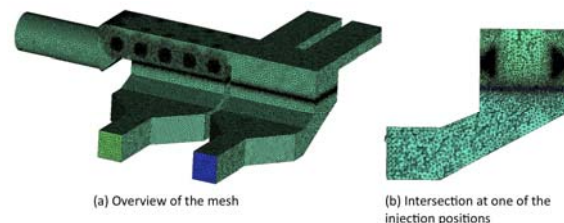


Figure 3: Mesh with 943k nodes.

Boundary conditions and simulation settings

The full Navier-Stokes equations are solved for the flow and following (Brouwer et al., 1996; Nguyen et al., 2008) the RANS $k-\epsilon$ model have been used to describe the turbulence in this initial study. The boundary conditions applied mimic typical process data of a grate-kiln plant. The mass flow settings from the outlets and inlets are the same in all simulations and all gases are treated as being ideal. An estimation of the kiln mass flow with an assumed leakage from the transition between kiln and grate has resulted in the assumed mass flow from the kiln. As mentioned earlier the geometry is simplified. In addition, the motion of the conveyor belt is neglected as well as the rotation and angle of the kiln.

The walls are modeled as smooth adiabatic walls implying that radiation and heat transfer to the bed and through the walls are neglected in the current model. The air channel inlet is set as a pressure inlet with a total pressure of 1atm with the flow direction normal to the boundary condition. For the other inlet and for the outlets mass flow is set at the boundary. Zero gradient is used as the turbulence option for fully developed turbulence at the inlets. When using a second order scheme time consuming simulations show a transient behavior in a small portion of the modeled volume. Instead most simulations were carried out with an upwind scheme that is believed to capture most features of the flow with a stationary assumption. Thermal heat transfer is modeled and the pressure drop over the porous pellet beds is dealt with by using an isotropic momentum loss and linear and quadratic resistance coefficients C_{R1} and C_{R2} according to a Forchheimer assumption, see Table 3. The boundary conditions for the inlets and the outlets can be seen in Figure 4.

Table 3: Linear and quadratic resistance coefficients.

| Zone | PH | TPH |
|----------|--------|--------|
| C_{R1} | 105.15 | 77.872 |
| C_{R2} | 145.34 | 128.15 |

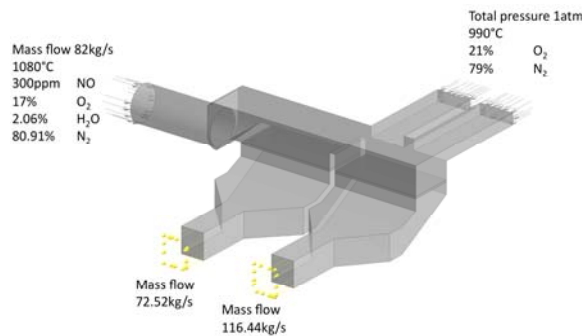


Figure 4: Default flow boundary conditions.

SNCR/Injection Settings

The simulations are carried out in such a way that the flow is computed neglecting the particles and then the particle equations are solved assuming that the particles do not influence the continuous phase except for the mass fraction that is two-way coupled. Furthermore the thermal energy heat transfer model was used with finite rate chemistry. The particles are one-way coupled with a Schiller Naumann drag force and a Ranz Marshall correlation for heat transfer. About 1000 droplets with a temperature of 26.85°C are injected at the sides of the PH-zone from each injection point. The mass flow of the reagent is changed depending on the reagent used and the molar ratio. The particle underrelaxation coefficients are set to 0.2 for energy, momentum and mass equations and temperature damping was used. The simulations were sensitive to the time step, so it was adapted to the case studied. The following parameters were varied when using urea

- Injection positions: 1, 2, 3, 4, 5
- Injection velocity: 10, 20, 50m/s
- Injection cone angle: 15, 30, 45°deg
- Particle diameter: 100, 300, 600µm
- NSR: 1, 2, 3

- Angle of injection direction

The default settings used for the reagent injection is seen in Table 4.

Table 4: Default settings for injection of reagent.

| Parameter | Ammonia | Urea |
|------------------------------|----------------|----------------|
| Injection positions | 1, 2 | 1, 2 |
| Injection velocity [m/s] | 20 | 20 |
| Injection cone angle [°deg] | 45 | 45 |
| Particle diameter [µm] | 200 | 300 |
| NSR | 2 | 2 |
| Angle of injection direction | normal to wall | normal to wall |
| Solution [wt%] | 25 | 32.5 |

The injection is always done from four lances each time, the positions evaluated can be seen in Figure 5.

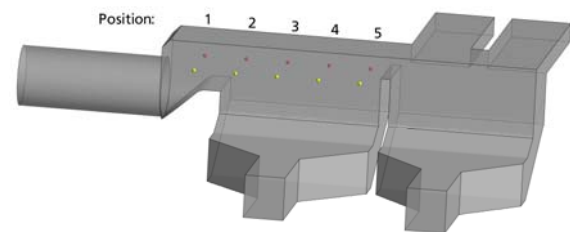


Figure 5: The different injection positions evaluated, the injection is always done from both sides.

RESULTS

Flow

When the flue gases from the kiln and the air from the air channels enter the grate the flow becomes complex. The flue gas from the kiln is spread over the PH-bed as seen in Figure 6 and swirls emanate from the beginning of the PH-zone in the upper part. The swirls have the highest velocity at the beginning of the zone and weaken when moving further into the zone as can be seen in Figure 7 and 8 and it will turn out that they have a large influence on where the reactions take place. The residence time becomes longer in the swirling regions and in the bulk down-stream closer to the TPH-zone.

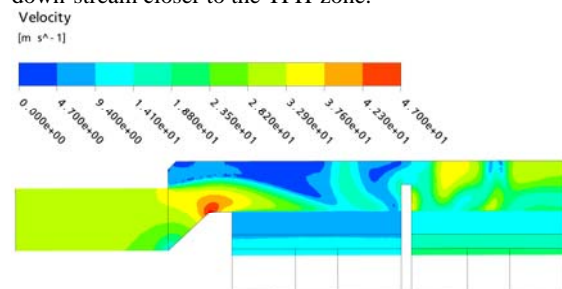


Figure 6: Velocity contours on a plane through the centreline of grate.

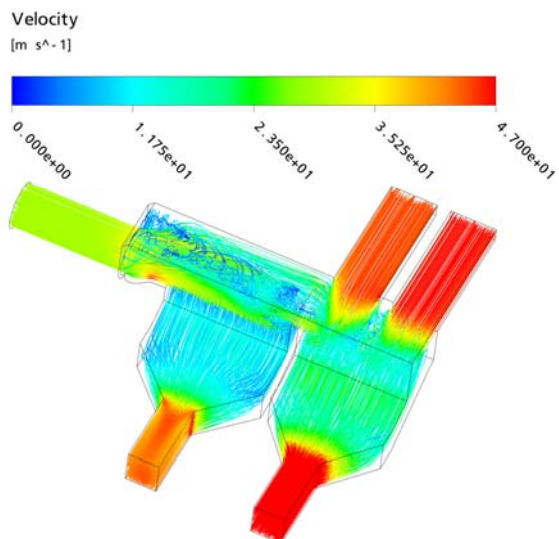


Figure 7: Streamlines coloured by velocity.

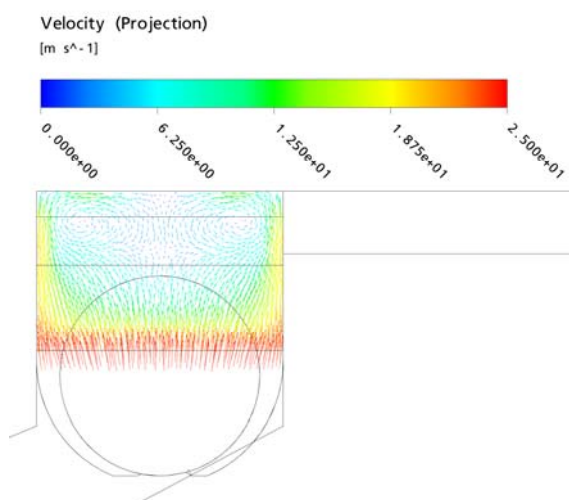


Figure 8: Velocity vectors on plane through the first injection position, seen from the TPH-zone.

Ammonia injection

No reduction is achieved when injecting ammonia, on the contrary a net production of NO is obtained. This is most probably due to the high temperature as well as the high oxygen level. The NO profile through the centreline of the grate can be seen in Figure 9.

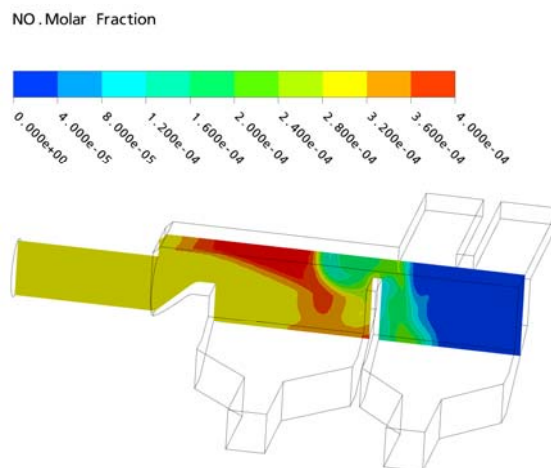


Figure 9: Plane through the centreline of grate.

Urea injection

Using urea as reagent resulted in a reduction of NO, which will be presented as the mass flow of NO going into the beds in the two zones compared to the mass flow of NO leaving the kiln. The result for the different parameters can be seen in Table 5.

Table 5: Summary of NO-reduction for varied parameters.

| Parameter | Settings | NO-reduction |
|---|---|-------------------------|
| Variation of injection positions | 45°deg, 300µm, 20m/s, NSR=2 | Position 1, 2 38.5 % |
| | | Position 2, 3 29.3 % |
| | | Position 3, 4 24.4 % |
| | | Position 4, 5 20.0 % |
| Variation of injection velocity | 45°deg, 300µm, NSR=2, position 1 and 2 | 10m/s 35.6 % |
| | | 20m/s 38.5 % |
| | | 50m/s 39.0 % |
| Variation of cone angle | 300µm, 20m/s, NSR=2, position 1 and 2 | 15°deg 38.2 % |
| | | 30°deg 38.5 % |
| | | 45°deg 38.5 % |
| Variation of particle diameter | 30°deg, 20m/s, NSR=2, position 1 and 2 | 100µm 27.4 % |
| | | 300µm 38.5 % |
| | | 600µm 35.1 % |
| Variation of NSR | 30°deg, 300µm, 20m/s, position 1 and 2 | NSR=1 24.6 % |
| | | NSR=2 38.5 % |
| | | NSR=3 42.6 % |
| Variation of angle of injection direction | 30°deg, 300µm, 20m/s, NSR=2, position 1 and 2 | Normal 38.5 % |
| | | Second 32.2 % |
| | | 45°deg up 32.2 % |
| | | Both 45°deg up |

The first result from the simulations is that urea should be injected as close to the inlet to the PH-zone as possible, see Figure 10. Otherwise the time for reaction becomes too short and a large part of the flue gases from the kiln has already passed through the bed earlier in the zone. The short reaction time gives high levels of H₂CO and N₂O at the inlet to the bed. The injection is therefore made from position 1 and 2 in further simulations.

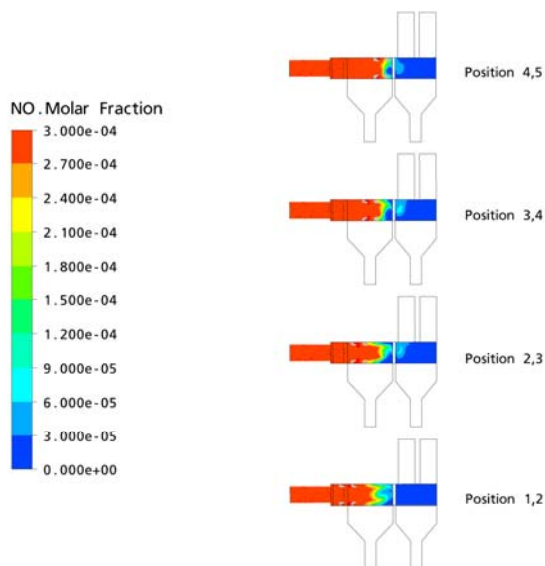


Figure 10: Contour of the NO molar fraction on a plane going through the inlet of the beds.

At the lowest velocity tested the momentum of the droplets is too small to get any significance penetration into the domain while the largest velocity results in adequate mixing but also more HNCO at the inlet to the bed since the particles from the second injection position nearly reaches the bed. There are also an uncertainty if a such high injection velocity can be reached in a full-scale plant therefore the medium injection velocity 20 m/s is used in the final sets of simulations. Notice that the reactions generated from the first injection position are accelerated by the swirls showed in Figure 8. With the particle size and injection velocity used the cone angle does not influence the NO-reduction or the concentration of HNCO/N₂O at the bed inlets. When varying the droplet size it can be concluded that the droplets with the size 100µm are swept along the wall of the continuous phase and the distance until the droplets are vaporized are short while with the largest droplets the reactions takes place close to the bed for the second injection point which gives high levels of HNCO and N₂O at the bed inlet as for the highest velocity of the droplets. In addition a normalized stoichiometric ratio ($NSR = 2n_{urea} / n_{NO}$, where n_{urea} is the injected moles of urea into the PH-zone and n_{NO} is the amount of moles NO coming from the kiln in the flue gases) gives a larger reduction but simultaneously a larger amount of HNCO and N₂O at the bed inlet.

CONCLUSIONS

A first model of SNCR-injection into a grate-kiln process has been successfully demonstrated. Although several simplifications are introduced on the geometry and on the description of the fluid flow it is shown that the flow in itself is complex. Main observations when adding the SNCR-technique are the short time available for reaction for urea and the slow decay of HNCO as the reactions leading to N₂O and CO can result in an increase of other emissions than NO such as N₂O.

The present model indicates that the SNCR- technique could be used in pelletizing plants with urea as reagent while ammonia fails. One reason for this may be that urea is better designed for the temperature and level of oxygen in a grate-kiln plant.

Caton and Xia (2004) concluded, for instance, that ammonia is suitable for low oxygen concentrations while cyanuric acid adapt to high oxygen concentrations and urea to intermediate values.

REFERENCES

- ALZUETA, M. U., BILBAO, R., MILLERA, A., OLIVA, M., & IBAEZ, J. C., (1998), "Interactions between Nitric Oxide and Urea under Flow Reactor Conditions", *Energy & Fuels*, **12**, 1001-1007.
- ANSYS CFX-SOLVER THEORY GUIDE, (2006), *Elsevier Academic Press*.
- BAULCH, D., COBOS, C., COX, R., ESSER, C., FRANK, P., JUST, T., ET AL., (1992), "Evaluated kinetic data for combustion modelling", *Journal of Physical and Chemical Reference Data*, **21**, 411-734.
- BIRKHOFF, F., MEINGAST, U., WASSERMANN, P., & DEUTSCHMANN, O., (2007), "Modeling and simulation of the injection of urea-water-solution for automotive SCR DeNOx-systems", *Applied Catalysis B: Environmental*, **70**, 119-127.
- BROUWER, J., HEAP, M. P., PERSHING, D. W., & SMITH, P. J., (1996), "A Model for Prediction of Selective Noncatalytic Reduction of Nitrogen Oxides by Ammonia, Urea, and Cyanuric Acid with Mixing Limitations in the Presence of Co", *Twenty-Sixth Symposium (International) on Combustion/The Combustion Institute*, 2117-2124.
- CATON, J. A., & XIA, Z., (2004), "The Selective Non-Catalytic Removal (SNCR) of Nitric Oxides From Engine Exhaust Streams: Comparison of Three Processes", *Journal of engineering for gas turbines and power*, **126**, 234-240.
- JAVED, M. T., IRFAN, N., & GIBBS, B., (2007), "Review Control of combustion-generated nitrogen oxides by selective non-catalytic reduction", *Journal of Environmental Management*, **83**, 251-289.
- LÖFFLER, G., SIEBER, R., HARASEK, M., HOFBAUER, H., HAUSS, R., & LANDAUF, J., (2005), "NO_x Formation in Natural Gas Combustion-Evaluation of Simplified Reaction Schemes for CFD Calculations", *Industrial and Engineering Chemistry Research*, **44**, 6622-6633.
- NGUYEN, T. D., LIM, Y.-L., KIM, S.-J., EOM, W.-H., & YOO, K.-S., (2008), "Experimental and Computational Fluid Dynamics (CFD) Simulation of Urea-Based Selective Noncatalytic Reduction (SNCR) in a Pilot-Scale Flow Reactor", *Energy & Fuels*, **22**, 3864-3876.
- ROTA, R., ANTOS, D., ZANOELO, É. F., & MORBIDELLI, M., (2002), "Experimental and modeling analysis of the NO_xOut process", *Chemical Engineering Science*, **57**, 27-38.
- WARNATZ, J., (1990), "NO_x Formation in High Temperature Processes", University of Stuttgart, Germany.
- WESTBROOK, C., & DRYER, F., (1984), "Chemical kinetic modeling of hydrocarbon combustion", *Progress in Energy and Combustion Science*, **10**, 1-57.